The Astrophysical Journal, 616:865–871, 2004 December 1

ANTARCTIC SUBMILLIMETER TELESCOPE AND REMOTE OBSERVATORY OBSERVATIONS OF ^{12}CO $J = 4 \rightarrow 3$ EMISSION FROM THE N44 COMPLEX IN THE LARGE MAGELLANIC CLOUD

Sungeun Kim,[1] Wilfred Walsh,[2] and Kecheng Xiao[2]
Received 2004 June 7; accepted 2004 August 11

ABSTRACT

We present Antarctic Submillimeter Telescope and Remote Observatory (AST/RO) observations of ^{12}CO $J = 4 \rightarrow 3$ and [C I] emission in the N44 H II complex in the Large Magellanic Cloud. We detected strong ^{12}CO $J = 4 \rightarrow 3$ emission toward the H II region known as N44BC, which is located on the rim of an expanding giant shell in the N44 region. Analysis with a photodissociation region model showed that the ^{12}CO $J = 4 \rightarrow 3$ emitting cloud is very dense, with $n_0 \approx 10^5$ cm^{-3}. We also note that there is a high-velocity component associated with the ^{12}CO $J = 4 \rightarrow 3$ emission. This probably originates from molecular material accelerated as a result of the motion induced by the expanding giant shell surrounding LH 47 in the N44 complex. We found that the kinetic energy of this high-velocity gas observed in the ^{12}CO $J = 4 \rightarrow 3$ emission toward the rim of the expanding H II shell is at least a factor of 4 higher than that derived for the H I and H II gas in this region.

Subject headings: galaxies: ISM — ISM: atoms — ISM: general — ISM: molecules — Magellanic Clouds — radio lines: galaxies

1. INTRODUCTION

The formation of molecular hydrogen plays a key role in star formation on all scales. We have learned over the last two decades that the interactions between atomic clouds and supernova remnants and/or stellar winds can provide a mechanism by which molecules can form (Elmegreen 1993). Furthermore, observations of atomic hydrogen in our Milky Way and nearby galaxies reveal the ubiquity of shells and supershells in the interstellar medium (ISM), indicating a potential origin for the substantial molecular material found in the ISM.

The Large Magellanic Cloud (LMC) presents us with a unique opportunity to study the interaction of massive stars and their interstellar environments that is perfectly illustrated by the *Spitzer* early-release observations of 30 Dor in the LMC.[3] First, the stars in the LMC are at a common distance and are close enough that individual stars and their stellar ejecta can be studied in great detail. Second, the LMC is inclined at only 27° to the line of sight, so that the three-dimensional structure of mass-loss bubbles can be mapped without problems of confusion. Third, the reddening is low in virtually all fields. Therefore, the LMC provides an excellent opportunity to study the effects of different levels of UV radiation from stars on their environments in the multiphase ISM, and it allows us to apply our understanding of the interstellar properties to studies of the early evolution of high-redshift and metal-poor galaxies.

At a distance of 55 kpc (Feast 1991), the LMC can be mapped with a high spatial resolution at high-excitation CO lines by the Antarctic Submillimeter Telescope and Remote Observatory (AST/RO). A recent [C I] and ^{12}CO $J = 4 \rightarrow 3$ study of the N159/N160 complexes in the LMC by Bolatto et al. (2000) elucidated the condition of the atomic and molecular medium in the early stages of star formation in this low-metallicity system. The dust-to-gas ratios are lower than those in the Milky Way, so UV radiation can penetrate deeper into the clouds and dissociate more CO molecules to greater depths in the LMC (Pak et al. 1998; Bolatto et al. 1999, 2000). The present study looked for dense molecular clouds in the swept-up material of the H I supershells in the LMC as support for self-propagating star formation (Elmegreen & Lada 1977; Dopita et al. 1985; Olsen et al. 2001) and found ^{12}CO $J = 4 \rightarrow 3$ emission toward the rim of the expanding giant H I and H II shells surrounding the OB association LH 47 (Lucke & Hodge 1970; Meaburn & Laspias 1991; Kim et al. 1998a). When compared to the CO $J = 1 \rightarrow 0$ emission (Cohen et al. 1988; Israel et al. 1993; Chin et al. 1997; Heikkilä et al. 1998; Fukui et al. 1999; Mizuno et al. 2001), this traces the massive core of the molecular clouds.

2. OBSERVATIONS

The observations were performed during the austral winter season of 2002 at AST/RO, located at 2847 m altitude at the Amundsen-Scott South Pole Station (Stark et al. 2001). This site has very low water vapor, high atmospheric stability, and a thin troposphere, making it exceptionally good for submillimeter observations (Chamberlin et al. 1997; Lane 1998). AST/RO is a 1.7 m diameter, offset Gregorian telescope that is capable of observing at wavelengths between 200 μm and 1.3 mm (Stark et al. 2001). The receivers used were a 230 GHz SIS receiver with 75–90 K double-sideband noise temperature and a dual-channel SIS waveguide receiver (Walker et al. 1992; Honingh et al. 1997) for simultaneous 461–492 GHz and 807 GHz observations with double-sideband noise temperatures of 320–390 K and 1050–1190 K, respectively. Telescope efficiency, η_l, estimated using moon scans, skydips, and measurements of the beam-edge taper, was ~90% at 230 GHz, 81% at 461–492 GHz, and 71% at 807 GHz.

Atmosphere-corrected system temperatures ranged from 200 to 400 K at 219–230 GHz, 700 to 4000 K at 461–492 GHz,

[1] Department of Astronomy and Space Science, Sejong University, KwangJin-gu, KunJa-dong 98, Seoul 143-747, Korea; skim@arcsec.sejong.ac.kr.

[2] Harvard-Smithsonian Center for Astrophysics, 60 Garden Street, MS-12, Cambridge, MA 02138.

[3] See *Spitzer* image at http://www.spitzer.caltech.edu/media/releases/ssc2004-01/index.shtml.

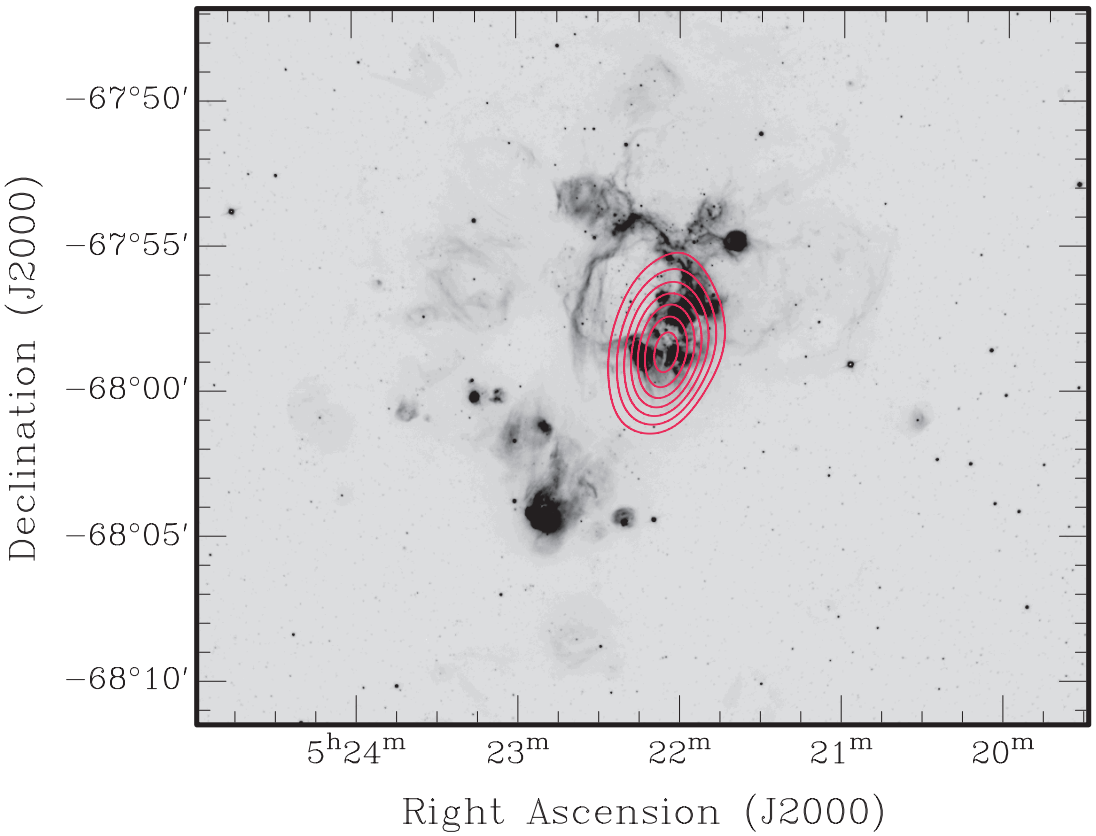

FIG. 1.—Integrated intensity contour map of ^{12}CO $J = 4 \rightarrow 3$ emission observed with AST/RO. The gray scale is the Hα image of the N44 complex (C. Smith 1998). The range of velocity integration is from 272 to 300 km s^{-1}. The lowest contour is 2.3 K km s^{-1}, and the contours increase by 1.0 K km s^{-1}.

and 9000 to 75,000 K at 807 GHz. A beam-switching mode was used, with emission-free reference positions chosen at least 20′ from the regions of interest, to make a small map of points surrounding DEM 152. These maps were repeated as often as required to achieve a suitable signal-to-noise ratio.

Emission from the ^{12}CO $J = 4 \rightarrow 3$ and CO $J = 7 \rightarrow 6$ lines at 461.041 and 806.652 GHz, together with the [C I] line at 492.262 GHz, was imaged over a 6′ square region centered on 5^{h}22^m, −67°58′ (J2000) with 0.′5 spacing; i.e., a spacing of half a beamwidth or less. AST/RO suffers pointing errors of the order of 1′, and the beam sizes (FWHM) were 103″–109″ at 461–492 GHz and 58″ at 807 GHz (Stark et al. 2001).

Two acousto-optical spectrometers (AOSs; Schieder et al. 1989) were used as back ends. The AOSs had 1.07 MHz resolution and 0.75 GHz effective bandwidth, resulting in velocity resolution of 0.65 km s^{-1} at 461 GHz and 0.37 km s^{-1} at 807 GHz. The data were then smoothed to a uniform velocity resolution of 1 km s^{-1}. The high-frequency observations were made with the CO $J = 7 \rightarrow 6$ line in the lower sideband (LSB). Since the intermediate frequency of the AST/RO system is 1.5 GHz, the $^3P_2 \rightarrow {}^3P_1$ line of [C I] appears in the upper sideband (USB) and is superposed on the observed LSB spectrum. The local oscillator frequency was chosen so that the nominal line centers appear separated by 100 km s^{-1} in the double-sideband spectra. A third AOS, used for only a few spectra, had 0.031 MHz resolution and 0.25 GHz bandwidth.

The standard chopper wheel calibration technique was employed, implemented at AST/RO by way of regular (every few minutes) observations of the sky and two blackbody loads of known temperature (Stark et al. 2001). Atmospheric transmission was monitored by regular skydips, and known bright sources were observed every few hours to further check calibration and pointing. At periodic intervals and after tuning, the receivers were manually calibrated against a liquid-nitrogen–temperature load and the two blackbody loads at ambient temperature and about 100 K. The latter process also corrects for the dark current of the AOS optical CCDs. The intensity calibration errors became as large as ±15% during poor weather periods.

The data in this survey were reduced using the COMB data reduction package. After elimination of scans deemed faulty for various instrumental or weather-related reasons (less than ∼10% of the total data set), linear baselines were removed from the spectra.

3. RESULTS

In Figure 1, we present a contour map of the ^{12}CO $J = 4 \rightarrow 3$ line emission taken with AST/RO overlaid on an Hα image. There is strong ^{12}CO $J = 4 \rightarrow 3$ emission detected at R.A. = 5^{h}22^{m}05.^{s}3, decl. = −67°58′41.″8 (J2000) that is associated with the N44 complex in the LMC. The interstellar complex N44 was found by Henize (1956) and is one of the largest complexes in the LMC. It consists of two giant Hα shells. "Shell 1" is prominent; the other one is fainter and located at the western side of Shell 1 (Meaburn & Laspias 1991). Shell 1 contains the OB association LH 47 (Lucke & Hodge 1970). The ^{12}CO $J = 4 \rightarrow 3$ emitting cloud is located along the western boundary of the giant Hα shell Shell 1 emission, as seen in Figure 1, and the peak of the ^{12}CO $J = 4 \rightarrow 3$ emission appears to be associated with the bright H II region N44BC ($\alpha_{1950} = 5^h22^m10.^s6$, $\delta_{1950} = -68°00'32''$). The N44 complex is one of the brightest CO $J = 1 \rightarrow 0$ emission regions in the LMC from the 1.2 m MINI telescope survey by Cohen et al. (1988) and the recent 4 m NANTEN survey by

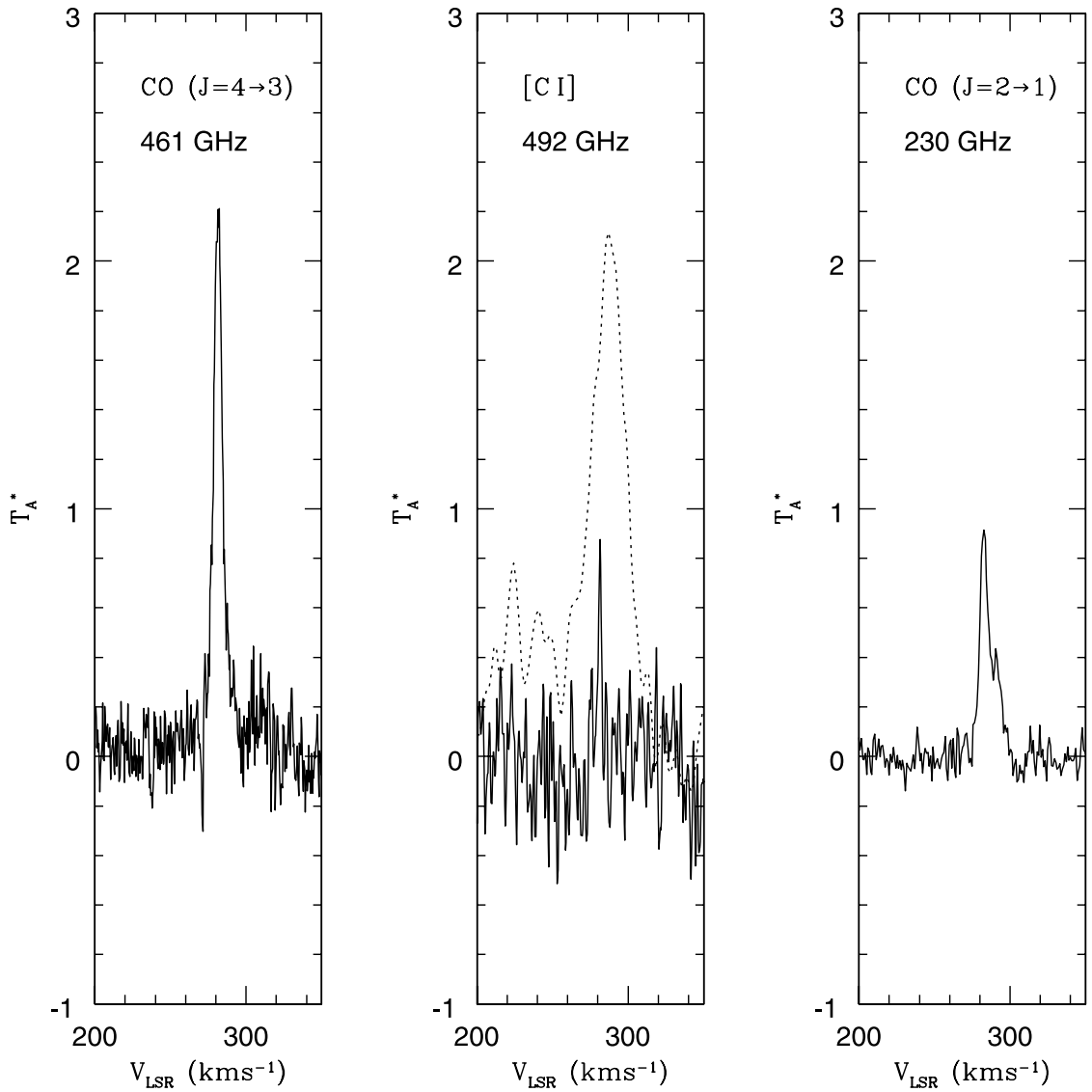

FIG. 2.—Spectra of ^{12}CO $J = 4 \rightarrow 3$, [C I] 492 GHz, and CO $J = 2 \rightarrow 1$ observed toward the peak of the ^{12}CO $J = 4 \rightarrow 3$ emission in the N44 complex. A Hanning-smoothed CO $J = 2 \rightarrow 1$ line profile is displayed for this position. The H I spectrum of this position is overlaid as a dashed line. The unit of the H I emission is multiplied by 0.1 and in Jy beam^{-1}.

Fukui et al. (1999) and Mizuno et al. (2001). DCO^+ emission has also been detected in N44BC (Chin et al. 1996).

Figure 2 presents the 461 GHz ^{12}CO $J = 4 \rightarrow 3$, 492 GHz [C I], and 230 GHz CO $J = 2 \rightarrow 1$ line profiles at the peak of the contour map at R.A. = $5^h22^m5\overset{s}{.}3$, decl. = $-67°58'41\overset{''}{.}8$ (J2000). The 461 GHz ^{12}CO $J = 4 \rightarrow 3$ emission from this region is bright, with $T_{MB} = 2.1$ K. The peak of the ^{12}CO $J = 4 \rightarrow 3$ emission appears at $V_{LSR} = 283.1$ km s^{-1}, as seen in Figure 2, which is similar to the H I systemic velocity at this position. The FWHM of ^{12}CO $J = 4 \rightarrow 3$ emission is 7.5 ± 0.1 km s^{-1}. This is somewhat narrower than the FWHM of H I emission, which is about 9 km s^{-1} (Kim et al. 1998a). Figure 3 shows the average spectrum for the entire AST/RO observation of the 461 GHz ^{12}CO $J = 4 \rightarrow 3$ emission and compares it to that of the 492 GHz [C I] emission line. We note a high-velocity component of ^{12}CO $J = 4 \rightarrow 3$ emitting molecular gas at $V_{LSR} \approx 304$ km s^{-1}, as seen in this figure. The average [C I] 492 GHz line profile over the entire AST/RO observation gives a much lower temperature for the [C I] line, $T_{MB} = 0.13$ K at $V_{LSR} = 283.1$ km s^{-1}. The line parameters for these spectra are given in Table 1. The luminosity L_{CO}, arising from the ^{12}CO $J = 4 \rightarrow 3$ emission, is about $3.73 \times 10^3\ L_\odot$, calculated as the product of the area and the integral of the mean global profile. The luminosity of ^{12}CO $J = 4 \rightarrow 3$ emission is close to that of the Sgr A complex (Kim et al. 2002). No lines were detected in CO $J = 7 \rightarrow 6$ emission and [C I] 809 GHz emission. However, an upper limit for the CO $J = 7 \rightarrow 6$ integrated intensity is derived as $\sim 1.5 \pm 0.2$ K km s^{-1} within this region where the ^{12}CO $J = 4 \rightarrow 3$ emission is detected. The upper limit is defined by 3 σ rms noise, and the rms noise in the integrated intensity of a nondetected region was calculated by $(n_{chan})^{1/2} \Delta v_{chan} T_{rms}$, where n_{chan} is twice the FWHM of the line in numbers of channels and Δv is the channel separation in km s^{-1}. The uncertainty in this upper limit can be brought up by noise fluctuation.

4. DISCUSSION

4.1. *Photodissociated Regions in the N44 Complex*

Hydrogen is the most abundant element in the universe, and hydrogen atoms also make up most of the interstellar matter

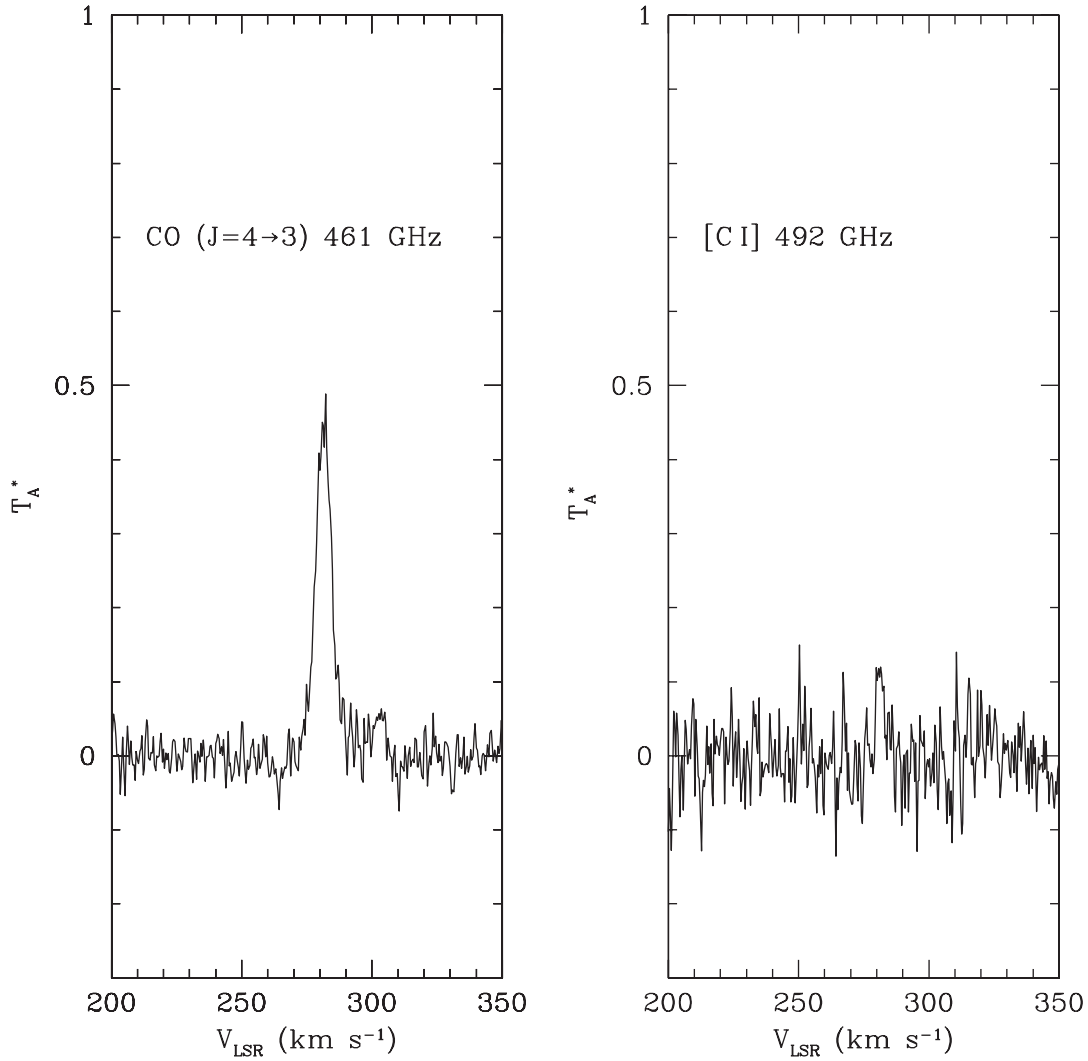

FIG. 3.—Spectra of ^{12}CO $J = 4 \rightarrow 3$ and [C I] 492 GHz averaged over the detected ^{12}CO $J = 4 \rightarrow 3$ emission in the N44 complex.

found in the LMC (Luks & Rohlfs 1992; Kim et al. 2003). A comparison of the ^{12}CO $J = 4 \rightarrow 3$ emission and H I emission from the N44 complex clearly shows that the position of peak brightness temperature in ^{12}CO $J = 4 \rightarrow 3$ emission corresponds to the region in which the H I emission is deficient, as seen in Figure 4. The H I image was made from an aperture synthesis survey of the LMC with the Australia Telescope Compact Array (ATCA; Kim et al. 1998b) and the Parkes single-dish survey (Staveley-Smith et al. 2003). The two surveys were combined using a Fourier-plane technique (Kim et al. 2003).

It is not yet possible to determine the ^{12}CO $J = 4 \rightarrow 3$ emission concentrations within the whole N44 complex in the LMC with our limited spatial coverage. However, our results show the detection of massive molecular clouds associated with the giant Hα shell within the N44 complex in the LMC. The observed ^{12}CO $J = 4 \rightarrow 3$ emission indicates that the neutral ISM toward the rim of the giant H II shell surrounding LH 47 in the N44 complex is very dense and warm, since the ^{12}CO $J = 4 \rightarrow 3$ transition requires $T > 50$ K and $n \sim 10^5$ cm^{-3} (Bolatto et al. 2000; Cecchi-Pestellini et al. 2001; Zhang et al. 2001).

The column density of neutral hydrogen, $N(\mathrm{H\ I}) = 1.822 \times 10^{18} \int T_b\, dv$ (Spitzer 1978), at the peak of the ^{12}CO $J = 4 \rightarrow 3$ emission was derived to be $\sim 3.4 \pm 0.1 \times 10^{21}$ cm^{-2}. By assuming that N44 giant shell Shell 1 is situated in the midplane

TABLE 1

OBSERVED LINE PARAMETERS

Line	T_{MB} (K)	V_{LSR} (km s^{-1})	ΔV (km s^{-1})	$\int T_{MB}\, dV$ (K km s^{-1})
230 GHz CO $J = 2 \rightarrow 1$	0.2 ± 0.005	282.6 ± 0.1	...	...
461 GHz ^{12}CO $J = 4 \rightarrow 3$	0.443 ± 0.004	283.165 ± 0.036	7.391 ± 0.082	3.484
492 GHz C I	0.126 ± 0.027	281.683 ± 0.327	3.130 ± 0.771	0.420
806 GHz CO $J = 7 \rightarrow 6$	...	...	...	1.5 ± 0.2

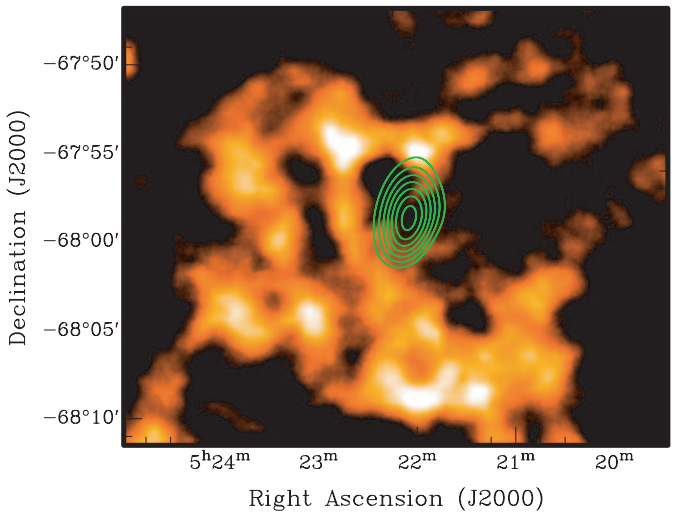

FIG. 4.—ATCA integrated H I image overlaid with ^{12}CO $J = 4 \rightarrow 3$ emission line contours, as described in Fig. 1.

of the LMC, we derived the volume density of the neutral hydrogen associated with the ^{12}CO $J = 4 \rightarrow 3$ emitting molecular cloud using the scale height of the LMC, which is approximately 180 pc (Kim et al. 1999). We found a volume density of neutral hydrogen associated with the ^{12}CO $J = 4 \rightarrow 3$ emission of $n_{\rm H} \approx 6.3 \pm 0.1$ cm^{-3}.

For comparison, we attempted to derive the density of hydrogen molecules, $n_{\rm H_2}$, in the ^{12}CO $J = 4 \rightarrow 3$ emitting gas in the N44 complex. As we have discussed above, the ^{12}CO $J = 4 \rightarrow 3$ emission traces the warm and dense molecular gas where collisional de-excitation balances radiative de-excitation (Spitzer 1978; Hollenbach & Tielens 1999). This usually occurs when the far-ultraviolet (FUV) photons from stars photodissociate the molecular cloud (Tielens & Hollenbach 1985; Sternberg & Dalgarno 1989; Wolfire et al. 1990; Hollenbach & Tielens 1999). The ^{12}CO $J = 4 \rightarrow 3$ emitting molecular cloud associated with the N44 complex is a fine example of a photodissociated region (PDR) in the LMC. The FUV photons ($6 < h\nu < 13.6$ eV) of stars in the OB association LH 47, enclosed by Shell 1 and a single ionizing star within N44C (Stasinska et al. 1986; Meaburn & Laspias 1991), are likely to be responsible for the photodissociation.

Using our newly observed line ratios of ^{12}CO $J = 4 \rightarrow 3$ and [C I] emission, the PDR model allows us to estimate the cloud density, kinetic temperature, and FUV fluxes of the gas (Tielens & Hollenbach 1985; Sternberg & Dalgarno 1989; Wolfire et al. 1990; Sternberg & Dalgarno 1995; Kaufman et al. 1999). This is illustrated in Figure 5, where the observed line ratios of the CO $J = 2 \rightarrow 1, J = 4 \rightarrow 3$, and [C I] 609 μm emission lines are plotted against the cloud density n and the incident FUV flux G_0, where G_0 is in units of the local interstellar value of 1.6×10^{-3} ergs cm^{-2} s^{-1} (Habing field). The estimate is given by the intersection of the tracks. The required particle density of H_2 is somewhat greater than 10^5 cm^{-3}. As the number density of the atomic hydrogen is only a few cm^{-3}, the estimated cloud density $n_{\rm H_2}$ from the PDR analysis indicates the density of hydrogen molecules in the cloud. We therefore suggest that the PDRs in the N44 complex contain about 1.7×10^5 hydrogen molecules cm^{-3}. However, this PDR model predicts G_0 to be too small, compared to the radiation field estimate for the cloud from LH 47, which is $G_0 = 100 \times (1 - f)/f$. A fraction $(1-f)$ of the radiation escapes the star-forming region and the enshrouding dust.

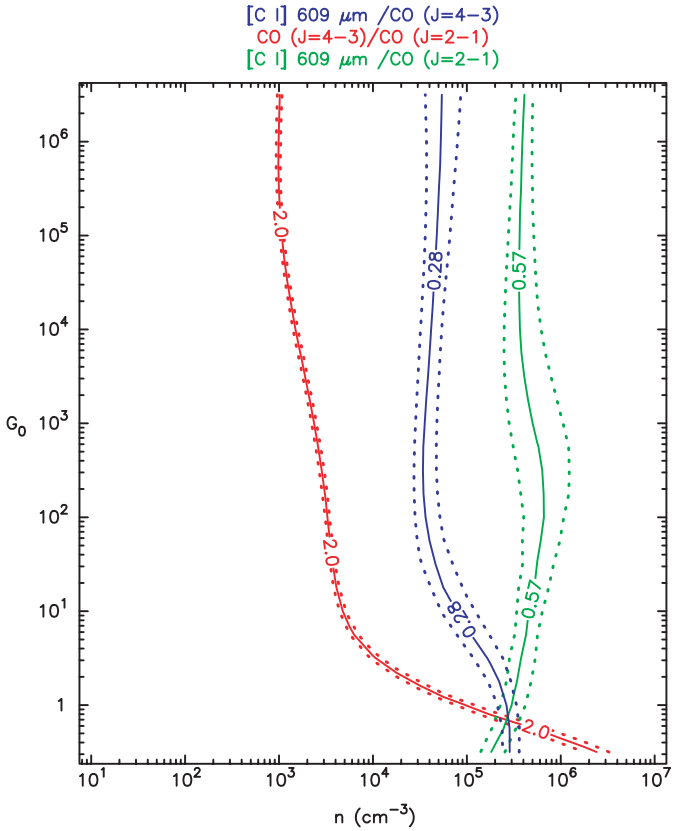

FIG. 5.—Line ratios of the ^{12}CO $J = 4 \rightarrow 3$, [C I] 492 GHz, and $J = 2 \rightarrow 1$ spectra observed with AST/RO plotted against an estimate of the cloud density n and incident FUV flux G_0, obtained using the PDR model. The error regions enclosed by dashed lines are computed from the errors of the line ratios.

This is in agreement with the results of Heikkilä et al. (1998), who found a cloud density of $n \approx 5 \times 10^5$ cm^{-3} toward the main molecular peaks in the region toward N44BC by multiline excitation analysis using their unpublished CS and SO data. It is not surprising to find such a high density of hydrogen molecules in the region associated with N44BC, where we detect the strong ^{12}CO $J = 4 \rightarrow 3$ emission. However, it is interesting to confirm the existence of very high density concentrations of molecular gas in the expanding H I and Hα shell. In addition, the present study has shown the extent of the dense gas as well as its location. A previous study by Chin et al. (1997) derived the molecular mass of N44BC, where we detect strong ^{12}CO $J = 4 \rightarrow 3$ emission, to be about $10^5\ M_\odot$ using the virial theorem. The mass of the ^{12}CO $J = 4 \rightarrow 3$ cloud can be derived using the following equation and assuming the LTE:

$$M_{\rm cloud} = \mu m({\rm H_2}) \Sigma D^2 \Omega N({\rm H_2}), \quad (1)$$

where D is the distance of the LMC, Ω is the solid angle subtended, $m(H_2)$ is the H_2 molecular mass, and μ is the mean molecular weight, assumed to be 1.36 by taking into account a relative helium abundance in mass. The H_2 column density, $N(H_2)$, can be derived from integrated CO $J = 2 \rightarrow 1$ intensity (in K km s^{-1}) and the CO-H_2 conversion factor $X = [N_{\rm H_2}/I_{\rm CO}] \sim (9 \pm 4) \times 10^{20}$ cm^{-2} (K km s^{-1})$^{-1}$ (Mizuno et al. 2001). Then the mass of molecular gas associated with N44BC is about $1.8 \pm 0.8 \times 10^6\ M_\odot$.

4.2. ^{12}CO $J = 4 \rightarrow 3$ *High-Velocity Gas?*

As clearly seen in Figure 3, there is a high-velocity component of ^{12}CO $J = 4 \rightarrow 3$ emission at $V_{\rm LSR} = 304$ km s^{-1}

arising from the molecular cloud that is associated with expanding H I and Hα shells (Meaburn & Laspias 1991; Magnier et al. 1996; Kim et al. 1998a). The brightness temperature of the high-velocity gas, T_{MB}, is about 0.1 K. This faint emission is probably the receding side of accelerated material with an expansion velocity of $v_{exp} \approx 20.9$ km s^{-1}. In this scenario, the high-velocity gas is presumed to be caused by the interaction of the molecular cloud with the stellar winds and/or supernova blasts of the hot stars in LH 47 (Lucke & Hodge 1970; Oey & Massey 1995). The expansion pattern of the H I gas shell surrounding LH 47 is similar to that of the ionized gas shell of Shell 1 (Kim et al. 1998a). The present study shows that the ^{12}CO $J = 4 \rightarrow 3$ emitting gas is accelerated with the velocity, which is only slightly smaller than the expansion velocity of the H I gas (30 km s^{-1}). We therefore expect that this high-velocity gas in the ^{12}CO $J = 4 \rightarrow 3$ emission is associated with the expanding atomic and ionized gas shells in the N44 complex. However, it is also conceivable that the H II region, N44BC, has driven a shock into the molecular cloud and produced such high-velocity molecular gas.

We estimate the mass of the high-velocity molecular cloud to be $3.0 \pm 1.3 \times 10^5$ $M_\odot$ by using the T_{MB} line ratio of the ^{12}CO $J = 4 \rightarrow 3$ emission at $V_{LSR} \sim 283$ km s^{-1} and $V_{LSR} \sim 304$ km s^{-1}. Thus, the kinetic energy of the high-velocity molecular cloud is approximately $1.3 \pm 0.6 \times 10^{51}$ ergs. This indicates a lower limit of the kinetic energy due to the solid angle of $\sim 5 \times 6$ arcmin^2 subtended by ^{12}CO $J = 4 \rightarrow 3$ emission. Assuming that this high-velocity molecular cloud is produced by an outward transfer of momentum from the expanding H I and H II shells, we calculate a lower limit on the total kinetic energy of the shell of 1.6×10^{51} ergs. We have summed the kinetic energy in the ionized gas shell and the H I shell for the superbubble Shell 1 in N44 (Kim et al. 1998a) and the lower limit of the kinetic energy of the high-velocity molecular cloud in N44. Adopting the thermal energy of Shell 1 (Chu & Mac Low 1990; Magnier et al. 1996; Kim et al. 1998a), we find that the summation of the lower limit of the total kinetic energy of the shell and its thermal energy appears to be 40% of the energy released by stellar winds and supernova explosions using the pressure-driven bubble model of Weaver et al. (1977).

5. CONCLUSIONS

We have presented the Antarctic Submillimeter Telescope and Remote Observatory (AST/RO) observations of ^{12}CO $J = 4 \rightarrow 3$ and [C I] emission in the N44 H II complex in the LMC. We detected strong ^{12}CO $J = 4 \rightarrow 3$ emission toward the H II region known as N44BC, which is located on the rim of an expanding giant shell in the N44 region. We note that there is a high-velocity component associated with the ^{12}CO $J = 4 \rightarrow 3$ emission with an expansion velocity of $v_{exp} \approx 20.9$ km s^{-1}, which is slightly smaller than that of the H I gas. This is likely to originate from molecular material accelerated as a result of the motion induced by the expanding giant shell surrounding LH 47 in the N44 complex.

We thank Antony A. Stark (AST/RO Principal Investigator), Adair P. Lane (AST/RO Project Manager), and C. Martin (2001 winterover) at the Smithsonian Astrophysical Observatory (SAO); C. Walker and his Steward Observatory Radio Astronomy Laboratory (SORAL) receiver group at the University of Arizona; J. Kooi and R. Chamberlin of Caltech, G. Wright of PacketStorm Communications, and K. Jacobs of Universität zu Köln for their work on the instrumentation; and R. Schieder, J. Stutzki, and colleagues at Universität zu Köln for their AOSs. We thank Marc Pound for helping us to use the Photodissociation Region Toolbox (PDRT). We thank C. Smith for his Hα image and You-Hua Chu for helpful discussion. We thank H I project team members Lister Staveley-Smith, Robert J. Sault, Mike Dopita, Ken C. Freeman, Dave McConnell, and Mike Kesteven. The referee offered many valuable suggestions that have also been incorporated. This research was supported in part by the National Science Foundation under a cooperative agreement with the Center for Astrophysical Research in Antarctica (CARA), NSF grant OPP-8920223. CARA is an NSF Science and Technology Center. Support was also provided by NSF grant OPP-0126090. S. K. was supported by Korea Science & Engineering Foundation (KOSEF) under a cooperative agreement with the Astrophysical Research Center of the Structure and Evolution of the Cosmos (ARCSEC).

REFERENCES

Bolatto, A., Jackson, J. M., Israel, F. P., Zhang, X., & Kim, S. 2000, ApJ, 545, 234
Bolatto, A., Jackson, J. M., Wilson, C. D., & Zhang, X. 1999, in IAU Symp. 190, New Views of the Magellanic Clouds, ed. Y.-H. Chu et al. (Cambridge: Cambridge Univ. Press), 128
Cecchi-Pestellini, C., Casu, S., & Scappini, F. 2001, MNRAS, 326, 1255
Chamberlin, R., Lane, A. P., & Stark, A. A. 1997, ApJ, 476, 428
Chin, Y.-N., Henkel, C., Millar, T. J., Whiteoak, J. B., & Mauersberger, R. 1996, A&A, 312, L33
Chin, Y.-N., Henkel, C., Whiteoak, J. B., Millar, T. J., Hunt, M. R., & Lemme, C. 1997, A&A, 317, 548
Chu, Y.-H., & Mac Low, M.-M. 1990, ApJ, 365, 510
Cohen, R. S., Dame, T. M., Garay, G., Montani, J., Rubio, M., & Thaddeus, P. 1988, ApJ, 331, L95
Dopita, M. A., Ford, H. C., & Webster, B. L. 1985, ApJ, 297, 593
Elmegreen, B. G. 1993, ApJ, 411, 170
Elmegreen, B. G., & Lada, C. J. 1977, ApJ, 214, 725
Feast, M. W. 1991, in IAU Symp. 148, The Magellanic Clouds, ed. R. Haynes & D. Milne (Dordrecht: Kluwer), 1
Fukui, Y., et al. 1999, PASJ, 51, 745
Heikkilä, A., Johansson, L. E. B., & Olofsson, H. 1998, A&A, 332, 493
Henize, K. G. 1956, ApJS, 2, 315
Hollenbach, D., & Tielens, A. G. G. M. 1999, Rev. Mod. Phys., 71, 173
Honingh, C. E., Haas, S., Hottgenroth, D., Jacobs, K., & Stutzki, J. 1997, Proc. 8th Int. Symp. on Space Terahertz Technology, ed. R. Blundell & E. Tong (Cambridge: CfA), 92
Israel, F. P., et al. 1993, A&A, 276, 25
Kaufman, M., Wolfire, M. G., Hollenbach, D. J., & Luhman, M. L. 1999, ApJ, 527, 795
Kim, S., Chu, Y.-H., Staveley-Smith, L., & Smith, R. C. 1998a, ApJ, 503, 729
Kim, S., Dopita, M. A., Staveley-Smith, L., & Bessell, M. 1999, AJ, 118, 2797
Kim, S., Martin, C., Stark, A. A., & Lane, A. P. 2002, ApJ, 580, 896
Kim, S., Staveley-Smith, L., Dopita, M. A., Freeman, K. C., Sault, R. J., Kesteven, M. J., & McConnell, D. 1998b, ApJ, 503, 674
Kim, S., Staveley-Smith, L., Dopita, M. A., Sault, R. J., Freeman, K. C., Lee, Y., & Chu, Y.-H. 2003, ApJS, 148, 473
Lane, A. P. 1998, BAAS, 30, 883
Lucke, P. B., & Hodge, P. W. 1970, AJ, 75, 171
Luks, T., & Rohlfs, K. 1992, A&A, 263, 41
Magnier, E. A., Chu, Y.-H., Points, S. D., Hwang, U., & Smith, R. C. 1996, ApJ, 464, 829
Meaburn, J., & Laspias, V. N. 1991, A&A, 245, 635
Mizuno, N., et al. 2001, PASJ, 53, 971
Oey, M. S., & Massey, P. 1995, ApJ, 452, 210
Olsen, K. A. G., Kim, S., & Buss, J. F. 2001, AJ, 121, 3075
Pak, S. J., Jaffe, D. T., van Dishoek, E. F., Johansson, L. E. B., & Booth, R. S. 1998, ApJ, 498, 735
Schieder, R., Tolls, V., & Winnewisser, G. 1989, Exp. Astron., 1, 101
Spitzer, Jr., L. 1978, Physical Processes in the Interstellar Medium (New York: Wiley)
Stark, A. A., et al. 2001, PASP, 113, 567
Stasinska, G., Testor, G., & Heydari-Malayeri, M. 1986, A&A, 170, L4

Staveley-Smith, L., Kim, S., Calabretta, M. R., Haynes, R. F., & Kesteven, M. J. 2003, MNRAS, 339, 87
Sternberg, A., & Dalgarno, A. 1989, ApJ, 338, 197
———. 1995, ApJS, 99, 565
Tielens, A. G. G. M., & Hollenbach, D. 1985, ApJ, 291, 747
Walker, C. K., Kooi, J. W., Chan, M., LeDuc, H. G., Schaffer, P. L., Carlstrom, J. E., & Phillips, T. G. 1992, Int. J. Infrared Millimeter Waves, 13, 785
Weaver, R., McCray, R., Castor, J., Shapiro, P., & Moore, R. 1977, ApJ, 218, 377
Wolfire, M. G., Tielens, A. G. G. M., & Hollenbach, D. 1990, ApJ, 358, 116
Zhang, X., Lee, Y., Bolatto, A., & Stark, A. A. 2001, ApJ, 553, 274